



## Methanol Promoted Oxidation of Nitrogen Oxide (NO<sub>x</sub>) by Encapsulated Ionic Liquids (ENILs)

Santiago, Ruben; Mossin, Susanne; Bedia, Jorge; Fehrmann, Rasmus; Palomar, José

*Published in:*  
Environmental Science and Technology

*Link to article, DOI:*  
[10.1021/acs.est.9b03103](https://doi.org/10.1021/acs.est.9b03103)

*Publication date:*  
2019

*Document Version*  
Peer reviewed version

[Link back to DTU Orbit](#)

*Citation (APA):*  
Santiago, R., Mossin, S., Bedia, J., Fehrmann, R., & Palomar, J. (2019). Methanol Promoted Oxidation of Nitrogen Oxide (NO<sub>x</sub>) by Encapsulated Ionic Liquids (ENILs). *Environmental Science and Technology*, 53(20), 11969-11978. <https://doi.org/10.1021/acs.est.9b03103>

---

### General rights

Copyright and moral rights for the publications made accessible in the public portal are retained by the authors and/or other copyright owners and it is a condition of accessing publications that users recognise and abide by the legal requirements associated with these rights.

- Users may download and print one copy of any publication from the public portal for the purpose of private study or research.
- You may not further distribute the material or use it for any profit-making activity or commercial gain
- You may freely distribute the URL identifying the publication in the public portal

If you believe that this document breaches copyright please contact us providing details, and we will remove access to the work immediately and investigate your claim.

## Methanol Promoted Oxidation of Nitrogen Oxide (NO<sub>x</sub>) by Encapsulated Ionic Liquids (ENILs)

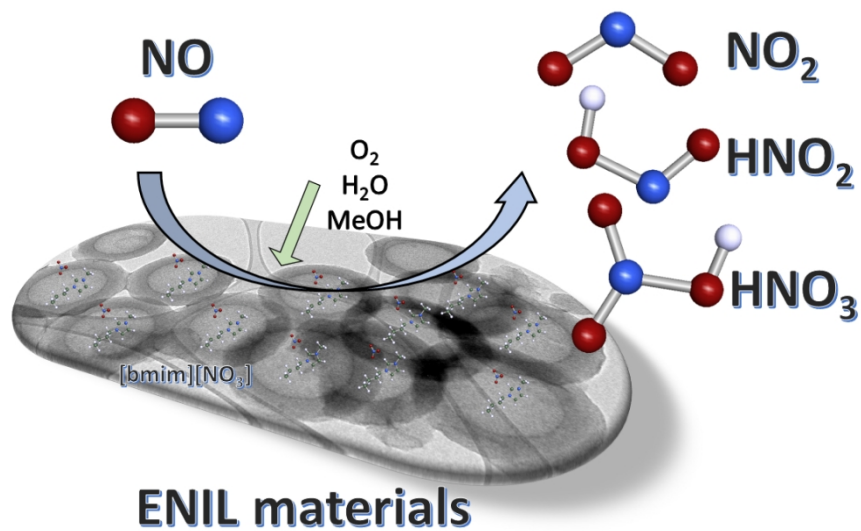
Ruben Santiago, Susanne Mossin, Jorge Bedia, Rasmus Fehrmann, and José Palomar

*Environ. Sci. Technol.*, **Just Accepted Manuscript** • DOI: 10.1021/acs.est.9b03103 • Publication Date (Web): 13 Sep 2019

Downloaded from [pubs.acs.org](https://pubs.acs.org) on September 24, 2019

### Just Accepted

“Just Accepted” manuscripts have been peer-reviewed and accepted for publication. They are posted online prior to technical editing, formatting for publication and author proofing. The American Chemical Society provides “Just Accepted” as a service to the research community to expedite the dissemination of scientific material as soon as possible after acceptance. “Just Accepted” manuscripts appear in full in PDF format accompanied by an HTML abstract. “Just Accepted” manuscripts have been fully peer reviewed, but should not be considered the official version of record. They are citable by the Digital Object Identifier (DOI®). “Just Accepted” is an optional service offered to authors. Therefore, the “Just Accepted” Web site may not include all articles that will be published in the journal. After a manuscript is technically edited and formatted, it will be removed from the “Just Accepted” Web site and published as an ASAP article. Note that technical editing may introduce minor changes to the manuscript text and/or graphics which could affect content, and all legal disclaimers and ethical guidelines that apply to the journal pertain. ACS cannot be held responsible for errors or consequences arising from the use of information contained in these “Just Accepted” manuscripts.



Methanol promoted oxidation of NO using Encapsulated Ionic Liquids (ENILs)

338x190mm (96 x 96 DPI)

# Methanol Promoted Oxidation of Nitrogen Oxide (NO<sub>x</sub>) by Encapsulated Ionic Liquids (ENILs)

Rubén Santiago<sup>1\*</sup>, Susanne Mossin<sup>2</sup>, Jorge Bedia<sup>1</sup>, Rasmus Fehrmann<sup>2</sup>, and  
José Palomar<sup>1</sup>

<sup>1</sup>Chemical Engineering Department. Universidad Autónoma de Madrid. 28049 Madrid.  
Spain

<sup>2</sup>Centre for Catalysis and Sustainable Chemistry, Department of Chemistry, Technical  
University of Denmark, DK-2800 Kgs. Lyngby (Denmark).

Corresponding author: ruben.santiago@uam.es

**Keywords:** NO oxidation; NO<sub>x</sub> removal; Ionic Liquids; ENIL; Flue gas

## Abstract

The removal of nitrogen oxides (NO<sub>x</sub>) has been extensively studied due to their harmful effects to health and environment. In this work, Encapsulated Ionic Liquids (ENILs) are used as catalysts for the NO oxidation at humid conditions and low temperatures. Hollow carbon capsules (C<sub>Cap</sub>) were first synthesized to contain different amounts of 1-butyl-3-methylimidazolium nitrate IL ([bmim][NO<sub>3</sub>]), responsible for the catalytic oxidation. Then, the materials were characterized using different techniques, by analyzing microstructure, porosity, elemental composition and thermal stability. The catalytic performance of ENIL materials was tested for NO conversion at different conditions. Thus, NO concentration was fixed at 2,000 ppm at dry and humid conditions. Then, the methanol promotion of the reaction was demonstrated, increasing the NO conversion values in all cases, and the alcohol/water ratio was optimized. The temperature effect was studied as well, using the optimal conditions based on the previous measurements. The results reflect that humid conditions do not have a negative effect in terms of NO conversion when using ENILs, opposite behavior as the observed for C<sub>Cap</sub> and traditional catalysts studied before. Low amount of IL inside the material (40% in mass) was found to be the optimum for the task, reaching conversions of almost 45% in near industrial conditions of temperature and O<sub>2</sub> and H<sub>2</sub>O concentrations in the flue gas with a GHSV = 10,000 h<sup>-1</sup>.

## 30 **Introduction**

31 Nitrogen oxides ( $\text{NO}_x$ ) are one of the major air pollutants from traditional electrical  
32 production as fossil fuel combustion, leading to well-known harmful effects <sup>1, 2</sup>. These  
33 negative effects comprise not only to the human health, causing important respiratory  
34 problems <sup>3</sup>, but also atmospheric pollution by acid rain, photochemical smog and ozone  
35 layer depletion <sup>4, 5</sup>. The major constituents of  $\text{NO}_x$  are nitrogen dioxide ( $\text{NO}_2$ ) and nitric  
36 oxide ( $\text{NO}$ ), which is an intermediate of the nitric acid synthesis in the chemical industry.  
37 Due to the low solubility of this gas in traditional solvents <sup>6</sup>, it is attractive to develop  
38 systems to remove or convert this compound into value-added or not harmful products.  
39 The most important technologies of the chemical industry to remove  $\text{NO}_x$  present in the  
40 flue gas are the well established SCR (selective catalytic reduction) and SNCR (selective  
41 non-catalytic reduction) of  $\text{NO}_x$  <sup>7, 8</sup>. However, these methods are not able to remove  $\text{NO}_x$   
42 completely because of some disadvantages during their use at high operating  
43 temperatures <sup>9</sup>, which also means high costs of the process. The catalysts typically used  
44 in SCR, mainly based on  $\text{V}_2\text{O}_5$ , work at temperatures above 300 °C <sup>10</sup>, taking advantage  
45 of the high temperatures of the power plants systems but placed in high dust position,  
46 promoting catalyst deactivation. However, other industrial units like waste incineration  
47 plants and ships demand also low temperature –end-of-pipe- de- $\text{NO}_x$  technologies.  
48 Therefore, research efforts have been centered on the development of new catalysts able  
49 to eliminate  $\text{NO}$  at lower temperatures. In this sense, not only the reduction process was  
50 taken into account, but others such as catalytic oxidation that was proved to work at lower  
51 temperature.

52 Several works were published in this field using zeolites <sup>11</sup> or carbonaceous  
53 materials <sup>12</sup> in presence of water at low temperature, giving as conclusion that the reaction  
54 occurs in the micropores of the material. Recently, an interesting work published by  
55 Ghafari *et al.* reports conversions up to 35 % of  $\text{NO}$  to  $\text{NO}_2$  in presence of water by using  
56 a polymer based catalyst at near room temperatures <sup>13</sup>. However, the presence of water  
57 decreased the polymer based catalysts performance. For this reason, it is important to  
58 develop catalysts are less affected in presence of water, or even with water as promoter  
59 to convert  $\text{NO}$  to value-added products.

60 Other alternatives to remove  $\text{NO}$  were also investigated, such as absorption <sup>14, 15</sup>. In  
61 this case, the absorption capacity of  $\text{NO}$  in aqueous solutions is reported to be low <sup>15</sup>. For  
62 these reasons, big efforts has been tried to enhancing this absorption capacity by means

63 of using additives <sup>16</sup>. Furthermore, it was detected the easy combination of NO with  
64 transition metals, so different metals were specifically designed for NO capture <sup>17</sup>. All  
65 these absorbents were aqueous solutions, limited by the low NO solubility in water <sup>18</sup>.

66 In last years, ionic liquids (ILs) are proposed as new chemical solvents, attracting a  
67 huge number of studies in e.g. gas capture applications <sup>19</sup>, due to their characteristic  
68 properties such as high absorption capacity, low vapor pressure and high thermal and  
69 chemical stability <sup>20</sup>, among others. Therefore, ILs have been extensively evaluated in gas  
70 capture, for instance of CO<sub>2</sub> <sup>21</sup>, SO<sub>2</sub> <sup>22</sup>, H<sub>2</sub>S <sup>23</sup>, NH<sub>3</sub> <sup>24</sup>, and volatile organic compounds <sup>25</sup>.  
71 It is remarkable that, however, few works on NO capture by ILs have been reported so  
72 far. Chen *et al.* <sup>26</sup> reported the first functional IL to capture NO, with the disadvantage of  
73 the high difficulty in the synthesis stage. Then, Sun *et al.* <sup>27</sup> synthesized a metallic  
74 functional ionic liquid able to chemically absorb NO. Recently, Kunov-Kruse *et al.* <sup>28</sup>  
75 reported that the IL 1-butyl-3-methylimidazolium nitrate ([bmim][NO<sub>3</sub>]) is a successful  
76 catalyst for NO oxidation into nitric acid in presence of water. However, it is well stated  
77 that the practical application of ILs are limited by their unfavorable transport properties  
78 <sup>29,30</sup>. In fact, several efforts have been centered on developing systems and materials able  
79 to reduce the kinetic control in the absorption operations based on ILs <sup>31-33</sup>. Thus,  
80 Supported Ionic Liquid Phase (SILP) concept was invented <sup>34-36</sup>. It consists of IL  
81 deposition in the pores of a solid support (silica, carbon, among others). In the case of gas  
82 capture application, these materials increase the mass transport rates compared with pure  
83 ILs due to the increase in the gas-liquid interfaces <sup>37</sup>. In the case of catalysis, it can be  
84 used like a solid heterogeneous catalyst for continuous fixed bed reactor systems <sup>35, 38</sup>.  
85 Recently, SILPs have been applied to different catalytic reactions. An efficient catalytic  
86 system based on metal ligand free in an environmental friendly IL system was  
87 successfully developed for Suzuki cross-coupling reactions <sup>39</sup>. Another metal/IL  
88 supported on nano-silica based catalysts were employed in the aldehyde C-H activation  
89 showing excellent yields of the desired aryl ketones <sup>40</sup>. Catalysts based on copper-doped  
90 silica supporting acidic ILs (based on [HSO<sub>4</sub>]<sup>-</sup> anion) demonstrated a good performance  
91 on Biginelly reaction <sup>41</sup>. In last years, CO<sub>2</sub> valorization has attracted the attention of the  
92 scientific community, using SILPs as catalysts for the reaction of cycloaddition of  
93 epoxides <sup>42,43</sup>. Regarding NO separation, the first approach using SILP materials (silica  
94 as support) was successfully applied by Fehrmann's group <sup>33</sup>. However, the IL loading  
95 can limit the practical application of gas capture <sup>32</sup>. A more recent alternative has

96 emerged: the Encapsulated Ionic Liquids (ENILs) concept, in which a high amount of IL  
97 (up to 80%) is contained inside hollow carbon capsules (internal diameter of 400-700 nm)  
98 with high specific surface area <sup>31</sup>. The performance of ENIL materials was tested by  
99 different gas capture applications such as ammonia <sup>31, 44</sup> and CO<sub>2</sub> in both physical <sup>30, 45</sup>  
100 and chemical <sup>46-48</sup> absorption. These works concluded that the encapsulation of the IL  
101 does not decrease absorption capacities and increase very significantly the absorption  
102 rates, due to the strong increase of contact surface after IL encapsulation. Furthermore,  
103 the nature of the IL does not significantly matter to the gas capture kinetics when using  
104 ENIL materials, since it is controlled by carbon capsule morphology [48]. Therefore,  
105 ENIL materials are able to solve the kinetic restrictions that pure ILs present in gas  
106 capture applications.

107 At this point, it emerged the idea of taking advantage of the improved mass transfer  
108 kinetics of ENIL materials for its application in NO oxidation by ionic liquid catalysis.  
109 Therefore, we propose 1-butyl-3-methylimidazolium nitrate ([bmim][NO<sub>3</sub>]) for its  
110 encapsulation into ENIL materials with different loadings. The IL selection was decided  
111 based on the previous work in which it was demonstrated that could be NO oxidized. The  
112 aim of this work is to evaluate the performance of a new support (based on hollow carbon  
113 capsules) in which the IL is encapsulated forming the ENIL materials in NO catalytic  
114 oxidation into NO<sub>2</sub>, HNO<sub>2</sub> and HNO<sub>3</sub> in presence of water at low temperatures.

## 115 **Experimental section**

### 116 *Materials*

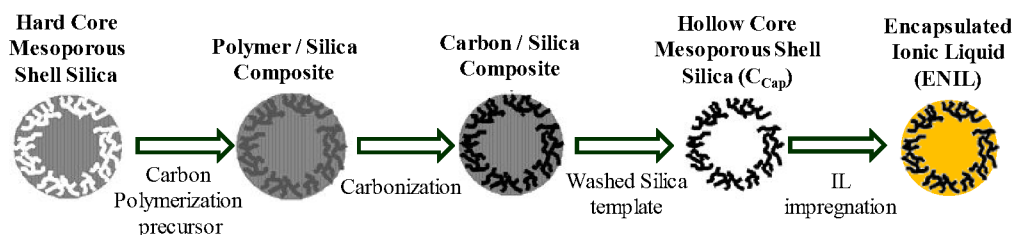
117 The IL 1-butyl-3-methylimidazolium nitrate (98 %) was purchased from Iolitec.  
118 The reagents used for hollow carbon capsules synthesis: phenol (99 %),  
119 paraformaldehyde (95-100 %), aluminum trichloride (95-100 %), ammonia (34 %) and  
120 absolute ethanol were supplied by Panreac. In addition, tetraethylorthosilicate (98 %)  
121 (TEOS), hexadecyltrimethoxysilane (90 %) (C16TMS) and hydrofluoric acid (48 %)  
122 were supplied by Sigma-Aldrich. Nitrogen, air and the mixture containing 10,000 ppmv  
123 of NO in nitrogen were supplied by AGA. The methanol (99.8 %) used for the promoted  
124 NO oxidation was supplied by Sigma-Aldrich.

### 125 *ENIL synthesis*

126 The hollow carbon capsules (C<sub>Cap</sub>) were synthesized as ENIL materials following  
127 the procedure reported by Büchel *et al.* <sup>49</sup>. This methodology has been successfully

128 applied by our group in the last years <sup>46, 48, 50, 51</sup> to obtain the  $C_{\text{Cap}}$  and then the ENIL  
 129 materials for their use in gas capture applications. The full description of the procedure  
 130 can be found in the referred works. In summary,  $C_{\text{Cap}}$  were synthesized following a  
 131 “templating” method in which the solid core and the mesoporous shell aluminosilicate  
 132 (SCMS) were used as template. The colloidal solution was maintained at 30 °C with  
 133 vigorous stirring to achieve homogenous diameters of the spheres. Then, the shell was  
 134 grown around the silica core by adding TEOS and C16TMS (to give porosity to the double  
 135 shell). After being filtrated and calcined at 550 °C, the SCMS was impregnated by a  
 136 phenolic resin (generated in situ) that will serve as carbon precursor (prior pyrolysis  
 137 stage). To accomplish this, aluminum trichloride was impregnated in the SCMS as  
 138 catalyst of the phenolic resin generation. Then, a mixture of paraformaldehyde and phenol  
 139 was added to completely impregnate the material generating the phenol-  
 140 paraformaldehyde resin. The resulting material could be heated until 160 °C that is the  
 141 curing temperature of the resin, during 5 hours and then increased until 850 °C under a  
 142 nitrogen atmosphere to accomplish the pyrolysis of the material. The resulting carbon  
 143 was washed with HF in order to remove the remaining silica present, being able to obtain  
 144 the final hollow carbon capsules ( $C_{\text{Cap}}$ ).

145 From  $C_{\text{Cap}}$ , the ENIL materials were prepared using incipient wetness impregnation.  
 146 400 mg of  $C_{\text{Cap}}$  were used and 1 mL of methanol-IL solution was added drop by drop  
 147 onto the carbon support. Then, the resulting ENIL materials were heated until 85 °C to  
 148 completely remove the remaining methanol. In this work, four different ILs loadings were  
 149 tested (20, 40, 60, and 80 % w/w). The complete synthesis process is shown in Scheme 1.  
 150 The methodology used was applied in several works of our group demonstrating the  
 151 homogenous distribution of the IL inside the  $C_{\text{Cap}}$  <sup>30, 44, 46-48</sup>.



152 Scheme 1: ENIL synthesis scheme

### 153 *ENIL characterization*

154 The  $C_{\text{Cap}}$  samples were characterized by means of elemental analysis in a LECO  
 155 CHNS-932 apparatus. The porous structure of the hollow spheres and ENIL materials



156 was also characterized by 77 K N<sub>2</sub> adsorption/desorption using a TriStar II 3020  
157 (Micromeritics) equipment after 10 h of degassing at 0.1 mbar and 393 K. The pore size  
158 distribution was calculated using t method. The microstructure and morphology of C<sub>cap</sub>  
159 were studied by transmission electron microscopy (TEM) using a JEOL JEM 2100 HT  
160 microscope. Then, the ENIL materials prepared were characterized by means of thermal  
161 gravimetric analysis (TGA) and elemental composition to check the amount of IL inside  
162 the material before and after reaction using a Mettler Toledo TGA/DSC 1 STARe system.  
163 This was carried out under a N<sub>2</sub> flow of 50 mL/min from room temperature until 600 °C  
164 with a heating rate of 10 °C/min.

#### 165 *NO oxidation measurements*

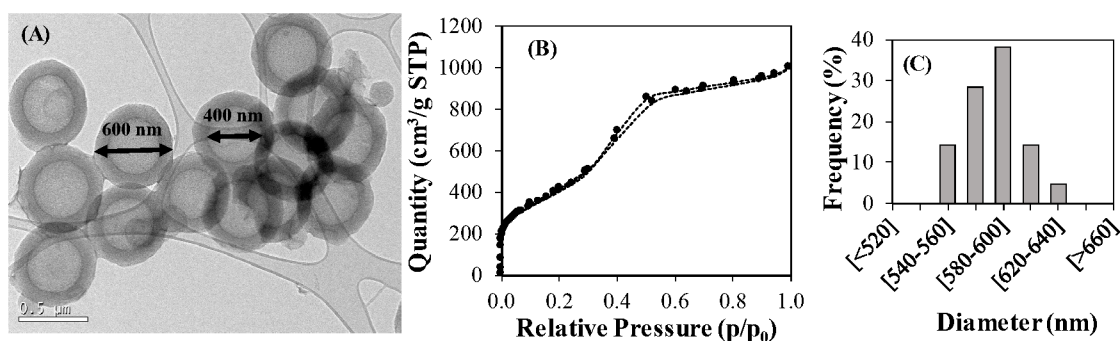
166 The prepared ENIL materials and hollow carbon spheres (C<sub>cap</sub>) were tested as NO  
167 catalysts using a fixed-bed reactor with ENILs volume of approximately 1.2 cm<sup>3</sup>,  
168 corresponding to masses between 0.4-1.0 g depending on the load of IL used. Most  
169 experiments were carried out at room temperature (near 24 °C). However, in the  
170 experiments in which the temperature was changed, the reactor was placed inside an oven  
171 able to control the temperature (regeneration experiments as well). A flue gas was passed  
172 through the reactor with a NO concentration of 2,000 ppm. The O<sub>2</sub> content was varied  
173 from 6.2 to 16.8 % and balanced with N<sub>2</sub>. Three mass flow controllers were used: i)  
174 connected to a 1% NO-N<sub>2</sub> bottle; ii) connected to an air bottle; iii) connected to a N<sub>2</sub>  
175 bottle. The total gas flow for each experiment was set at 200 mL/min. All the reactions  
176 were conducted at atmospheric pressure. Furthermore, the top of the reactor was fitted  
177 with a three-way valve that allows introducing the gases and the liquid inside the fixed-  
178 bed reactor. The flow of the liquid was controlled by a NE-300 Syringe Pump. In this  
179 sense, the relative humidity (RH) of the flue gas was changed and studied from 10 to 75  
180 % utilizing a syringe filled of deionized water. The addition of the methanol to promote  
181 the oxidation reaction was accomplished by adding a water/methanol solution to the  
182 system by the Syringe Pump. The methanol concentration (varied from 100 to 1600 ppm)  
183 and the flow rate needed were calculated in each experiment in order to maintain the  
184 desired conditions. The bottom of the reactor was conducted into a gas cuvette inside a  
185 Thermo Scientific Evolution 220 UV-Visible Spectrophotometer. Each measurement  
186 collects the whole spectrum from 200 to 600 nm. NO have absorption bands in the ultra-  
187 violet (UV) region at 204 nm, 215 nm and 226 nm. This last peak was used to quantify  
188 the NO in the exit of the reactor and calculate the conversion. Peakfit.m matlab script was

189 used for deconvolution of the three peaks, using last one at 226 nm to calculate  
 190 conversions as a function of the peak area using a standard curve performed with different  
 191 NO concentrations mixed with an inert gas ( $N_2$ ). Other peaks that could be identified in  
 192 the spectra are due to  $NO_2$  having a broad peak around 405 nm and  $HNO_2$  that presents  
 193 four different peaks from 340 to 390 nm; and the  $HNO_3$  exhibiting a broad peak in the  
 194 NO region (from 200 to 250 nm). These peaks can indicate which species are being  
 195 formed depending on the operation conditions tested. In all cases, the conversion was  
 196 calculated at steady state, i.e. identical spectra obtained during at least 2 hours. Before  
 197 changing the relative humidity of the inlet gas, the desorption experiment was carried out  
 198 after heating the sample up to 130 °C using 100 mL/min of  $N_2$  in presence of water (ratio  
 199 1:1) to totally remove the water, methanol and nitric acid present in the sample.

## 200 Results

### 201 $C_{Cap}$ and ENILs characterization

202 The hollow carbon capsules ( $C_{Cap}$ ) and the four prepared ENIL materials were  
 203 characterized by means of microscopy, pore structure, elemental analysis and thermal  
 204 stability. Thus, Figure 1A shows TEM microscopy image of the  $C_{cap}$  while Figure 1C  
 205 shows the size distribution of the analyzed sample by several TEM images. Figure 1B  
 206 presents the  $N_2$  adsorption-desorption isotherm of the  $C_{Cap}$  before the incorporation of  
 207 [bmim][ $NO_3$ ] IL.



208 Figure 1: (A) TEM image of the hollow carbon capsules ( $C_{Cap}$ ) to prepare ENIL materials;  
 209 (B)  $N_2$  adsorption/desorption isotherms @ 77 K of  $C_{Cap}$  and (C) size distribution of  $C_{Cap}$

210 Figure 1A shows the homogenous size distribution of the material with spherical  
 211 shape and an external diameter of almost 600 nm with a shell thickness of 200 nm and a  
 212 large central hole. The  $N_2$  adsorption-desorption isotherm (Figure 1B) is typical of a  
 213 mesoporous material with a significant microporosity contribution (both as a consequence

214 of the porosity of the shell). Table 1 reflects the elemental analysis and the summarized  
 215 information extracted from the N<sub>2</sub> adsorption-desorption isotherms.

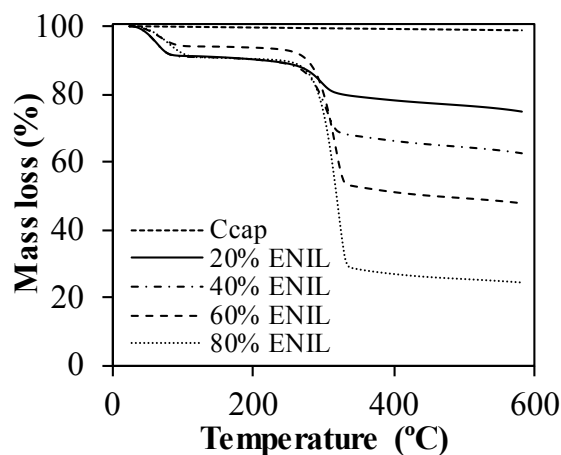
216

217 Table 1: Carbon capsules (C<sub>cap</sub>) characterization by means of elemental analysis and N<sub>2</sub>  
 218 adsorption-desorption @ 77 K.

Characterization technique			
Elemental Analysis		N <sub>2</sub> adsorption-desorption	
% C (w)	91.40	S <sub>BET</sub> (m <sup>2</sup> /g)	1,494
% H (w)	1.80	V <sub>micropore</sub> (cm <sup>3</sup> /g)	0.55
% N (w)	0.10	V <sub>mesopore</sub> (cm <sup>3</sup> /g)	0.68
		Pore size (Å)	41.35

219

220 The elemental analysis extracted from Table 1 confirm the carbonaceous nature of  
 221 the material (more than 90% of carbon). The incorporation of the different amounts of IL  
 222 in the support is possible due to the high porosity. The material possesses both  
 223 mesoporosity and microporosity mainly based on the porous shell grown around the  
 224 central hollow core. Thus, the average pore size is almost 40 Å, which reflects the  
 225 mesoporosity of the material. In that way, the different amounts of IL can be incorporated  
 226 in the support filling the double shell first (until 40% of IL) and the large central hole  
 227 afterwards<sup>31</sup>. Once the C<sub>cap</sub> was synthesized and characterized, the ENIL materials can  
 228 be prepared with different amounts of IL. In order to check the amount of IL incorporated  
 229 in each sample, Figure 2 shows the TGA analysis of each one.

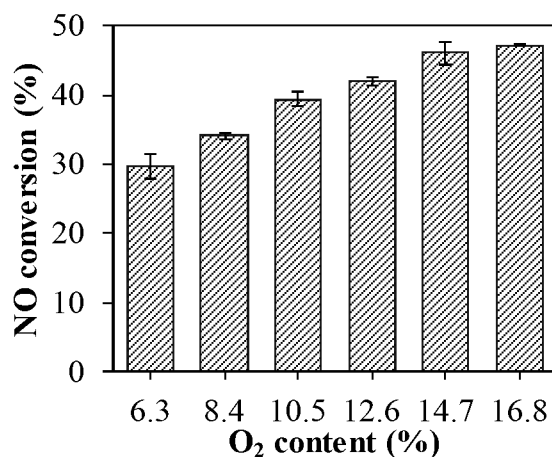


230 Figure 2: TGA analysis of the materials used in this work: hollow carbon capsules (C<sub>cap</sub>)  
 231 and ENIL materials with four different IL loading (20, 40, 60 and 80 % of [bmim][NO<sub>3</sub>]).  
 232 Analysis carried out with a temperature increase of 10 °C·min<sup>-1</sup> under 50 mL·min<sup>-1</sup> of N<sub>2</sub>.

233 Starting with the TGA analysis of  $C_{\text{Cap}}$ , as can be seen in Figure 2, our support is  
 234 stable at least until 600 °C under nitrogen. Therefore, using this curve as reference, it is  
 235 possible to estimate the amount of IL present in each sample taking into account the  
 236 remaining mass at 600 °C (attributed to the carbon support). In all cases, after a little  
 237 decay prior to 100 °C (possible sorbed water) the final value corresponds perfectly to the  
 238 nominal amount of each material. The elemental composition results of each material (see  
 239 Table S1 of Supplementary Information) confirm the conclusions of TGA analysis. In  
 240 addition, the pore size distribution of all the ENIL materials are shown on Figure S1 of  
 241 the Supplementary Information confirming almost the same average pore size (40 Å) but  
 242 decreasing the pore volume by increasing the IL load on ENILs. The experimental  $N_2$   
 243 adsorption/desorption isotherms are also included in Figure S2 of Supplementary  
 244 Information. An increase in the IL loading inside ENIL material leads to the filling of the  
 245 pores until 60-80%, in which all remained completely occupied or blocked by IL <sup>31,32</sup>.

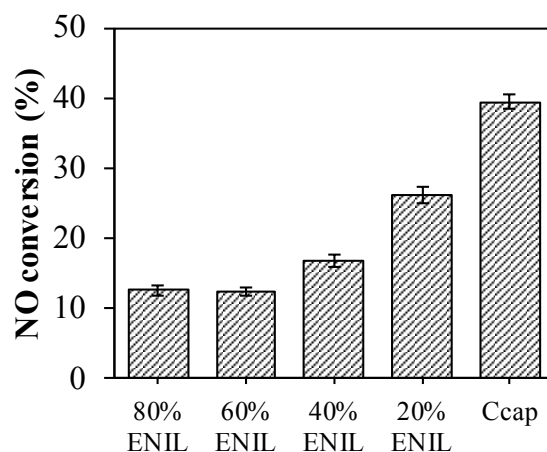
#### 246 *NO oxidation in dry conditions*

247 The different prepared catalysts were first tested in absence of moisture. Prior to  
 248 test the ENIL materials performance in NO catalytic oxidation, it is important to  
 249 understand the behavior of the support ( $C_{\text{Cap}}$ ) under different oxidation conditions. Figure  
 250 3 shows the NO conversion in the hollow carbon capsules using different  $O_2$  contents. In  
 251 this case, the reaction involved in experiments in dry oxygen condition is depicted in  
 252 Eq. 1.



254 Figure 3: NO conversion of hollow carbon capsules ( $C_{\text{cap}}$ ) in dry conditions at different  
 255 oxygen contents. Gas composition: 2,000 ppm NO, 6.3-16.8%  $O_2$ , balance  $N_2$ , Flow:  
 256 200  $\text{mL} \cdot \text{min}^{-1}$ , GHSV=10,000  $\text{h}^{-1}$ . Experiments conducted at room temperature.

257 As can be seen, the trend clearly shows higher catalytic activity by increasing the  
258 amount of O<sub>2</sub> in the system, reaching almost 48 % of conversion at 16.8% of O<sub>2</sub>. This  
259 means that the presence of more O<sub>2</sub> in the system leads to the formation of more NO<sub>2</sub>,  
260 resulting in higher conversion values (see Figure S3 in Supporting Information).  
261 Compared to those previously reported in the literature, we used 10.5% O<sub>2</sub> (almost 40 %  
262 NO conversion) which corresponds to those applied at industrial conditions to treat almost  
263 2,000 ppm of NO<sup>52</sup>. Zeolite based catalysts exhibit NO conversions from 5 to 45 %<sup>11</sup>  
264 depending on the modifications carried out, concluding that those with higher micropore  
265 volume show the greatest performance. Zhang *et al.*<sup>12</sup> reported NO conversions up to 57  
266 % using microporous activated carbons. Sousa *et al.*<sup>53</sup> used doped carbons reaching  
267 conversions up to 75 % in the best case. In view of all these results, our C<sub>Cap</sub> material,  
268 later used as support for ENIL materials, presents NO conversion in dry O<sub>2</sub> conditions in  
269 the range of the zeolite catalysts and slightly lower when compared with activated carbons  
270 prior to their modification at almost same conditions. These differences may be attributed  
271 to the different porous structure of the materials. It is believed and proved that a high  
272 microporous structure leads to higher conversions. In the case of our material, it is  
273 basically a mesoporous material but presenting high micropore volume (see Table 1). The  
274 C<sub>Cap</sub> performance can be compared with the ENIL catalysts at 10.5% of O<sub>2</sub>. In Figure 4,



275 the NO conversion reached by each material (including the previous discussed C<sub>Cap</sub>) are  
276 compared.

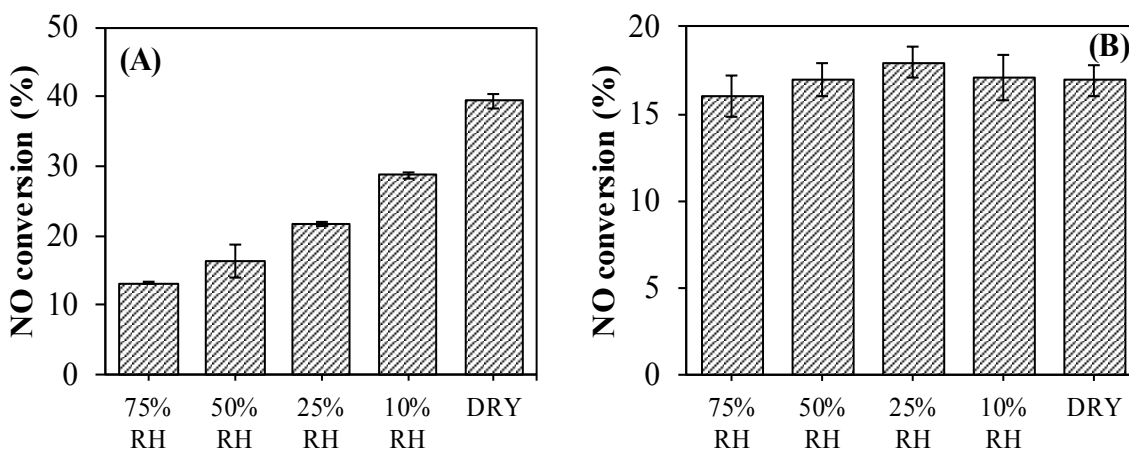
277 Figure 4: NO conversion of the different materials of the work in dry conditions. Gas  
278 composition: 2,000 ppm NO, 10.5% O<sub>2</sub>, balance N<sub>2</sub>, Flow: 200 mL·min<sup>-1</sup>,  
279 GHSV=10,000 h<sup>-1</sup>. Experiments conducted at room temperature.

280 As can be seen, NO conversion decreases by increasing the amount of IL in the  
281 catalyst until the conversion remains constant (from 60% IL loading). This could be

282 explained due to filling of the pores of the  $C_{\text{Cap}}$  material (see the reduction in BET area  
 283 while increasing the IL loading in Table S1 of the Supplementary Information). In the  
 284 case of 20% and 40% ENIL material, the higher conversion may be attributed to partly  
 285 filled pores exhibiting more efficient IL distribution on the pore surface. From the  
 286 previous reported data with [bmim][NO<sub>3</sub>] IL<sup>28</sup>, it seems that the presence of water is key  
 287 leading to the formation of more [NO<sub>3</sub>]<sup>-</sup> anions (anion part of the IL) that may improve  
 288 the NO removal.

### 289 *NO oxidation in wet gas*

290 In order to simulate near industrial conditions the catalytic performance of our  
 291 materials was investigated in gas streams that contain around 10% O<sub>2</sub> and water.  
 292 Experiments in wet conditions follow the reaction of Eq. 2. More details about the  
 293 mechanism of NO oxidation reaction in presence of water using [bmim][NO<sub>3</sub>] can be  
 294 found in previous works<sup>28,54</sup>.

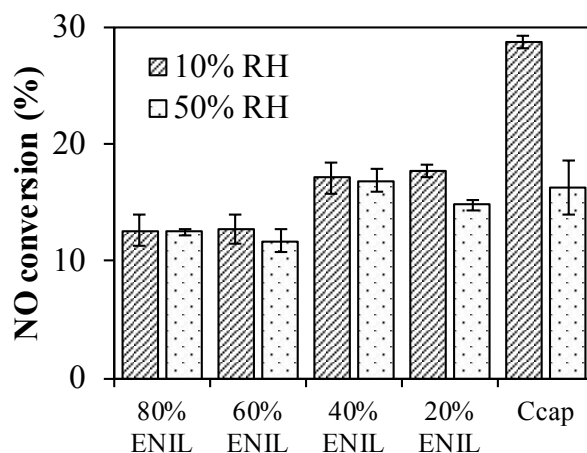


296 Figure 5: NO conversion of (A) the hollow carbon capsules ( $C_{\text{cap}}$ ) and (B) the 40 %  
 297 [bmim][NO<sub>3</sub>] ENIL material in different dry and wet conditions (from 10 to 75% Relative  
 298 Humidity). Gas composition: 2,000 ppm NO, 10.5% O<sub>2</sub>, balance N<sub>2</sub>, Flow: 200 mL·min<sup>-1</sup>,  
 299 GHSV=10,000 h<sup>-1</sup>. Experiments conducted at room temperature.

300 Figure 5A clearly shows the catalytic inhibition when water was added into the  
 301 system employing  $C_{\text{cap}}$  as catalyst. NO conversion reaches only a value of 13% at 75%  
 302 RH. This may be explained by the decrease of the NO adsorption mainly caused by the  
 303 competitive water adsorption. Some works reported that water affects negatively the NO  
 304 oxidation using activated carbons (AC) or zeolites. They reached the same conclusion:  
 305 the NO oxidation inhibition in presence of water is caused by adsorption competition.

306 Thus, Mochida *et al.*<sup>55</sup> showed a huge decrease in conversion by increasing RH in AC  
307 catalysts. Another work by Mochida *et al.*<sup>56</sup> showed the limitation of RH > 60% to the  
308 NO oxidation using AC catalysts. Guo *et al.*<sup>57</sup> reported the complete stop in NO oxidation  
309 when RH is higher than 20% using AC catalysts. The moisture influence was also studied  
310 in zeolite based catalysts<sup>58</sup> reaching conversions of only 10% when 8% of H<sub>2</sub>O is present  
311 in the flue gas stream, showing a dramatic inhibiting effect in that kind of catalysts. The  
312 most recent study at wet conditions concerns a new polymer based catalyst<sup>13</sup> in which  
313 the inhibition was also demonstrated when 50% RH was employed. In addition, we  
314 believe that the inhibition may also be caused by means of *capillary condensation*,  
315 described by the Kelvin equation<sup>59</sup>. At the pore diameter of C<sub>Cap</sub> (about 41 Å, see Table  
316 1), *capillary condensation* at room temperature is expected to occur at a RH around 50-  
317 60%<sup>60</sup> and may thus cause the observed deactivation in Figure 5A for RH > 50%. This  
318 phenomenon definitely does not occur when the IL is completely filling the pores of the  
319 support. As can be seen, the presence of water does not inhibit the NO oxidation when  
320 using ENIL material. This may be explained by the different NO oxidation mechanism  
321 by the [bmim][NO<sub>3</sub>] catalyst in presence of water that leads to conversion to HNO<sub>3</sub>  
322 instead of NO<sub>2</sub> in the dry gas as concluded in the previous work<sup>28</sup>. A slight increase in  
323 the HNO<sub>3</sub> and decrease in the NO<sub>2</sub> regions of the UV-Vis spectrum (see Figure S2 in  
324 Supporting Information) was thus found by adding water to the system compared to the  
325 C<sub>Cap</sub> catalyst. Therefore, this IL catalyst the first reported NO oxidation catalyst that is  
326 not negatively affected by presence of water.

327 Figure 6 shows the NO conversion of the studied materials at two different gas  
328 humidity levels.



329 Figure 6: NO conversion of the different materials at two different wet conditions (10 and  
330 50% Relative Humidity). Gas composition: 2,000 ppm NO, 10.5% O<sub>2</sub>, balance N<sub>2</sub>, Flow:  
331 200 mL·min<sup>-1</sup>, GHSV=10,000 h<sup>-1</sup>. Experiments conducted at room temperature.

332 For 10% RH, it can be seen that the C<sub>Cap</sub> material exhibits the highest conversion  
333 compared to the ENILs. It seems therefore the water levels are not enough for the ENIL  
334 materials to exhibit a decreased performance. The conversion follows almost the same  
335 trend as observed for the dry experiments, i.e. the NO conversion decreases while  
336 increasing the amount of IL in the material until 60% loading above, which it remains  
337 constant. However, a closer look reveals that the presence of water in the gas for the 20%  
338 ENIL catalyst seems to be partially inhibited compared to dry conditions, as in the case  
339 for the C<sub>Cap</sub>. This may mean that there are still some pores not completely filled with the  
340 IL.

341 Analyzing the 50% RH exposure, the presence of available pores for NO oxidation  
342 in the case of 20% ENIL material seems obvious due to the observed reduction in the NO  
343 conversion (but to a lesser extent than for C<sub>Cap</sub>) when compared with 10% RH exposure.  
344 This behavior was also concluded in terms of available pores while increasing the amount  
345 of ILs in the support by Lemus *et al.*<sup>31, 32</sup>. The rest of the materials exhibit unaltered  
346 behavior, since their activities are not affected by the addition of more water. If we now  
347 compare the performance of the materials at 50% RH, it can be seen that the 40% ENIL  
348 exhibits slightly higher NO conversion than C<sub>Cap</sub>, probably due to the difference in  
349 mechanism, while the 20% ENIL material shows almost the same behavior as C<sub>Cap</sub>,  
350 followed closely by the other two ENILs. Thus, it can be concluded that flue gas streams  
351 that contain high amount of water does not affect the ENIL materials performance (in  
352 terms of NO conversion), in contrast to the typical carbon materials (C<sub>Cap</sub>), in which the  
353 reaction is strongly inhibited.

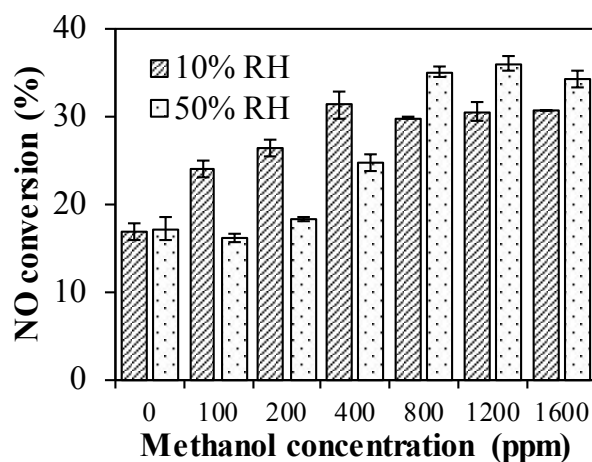
#### 354 *Methanol promoted NO oxidation in wet gas*

355 In the 1990's, methanol promoted NO oxidation at high temperatures (from 700 °C  
356 up to 1,000 °C) was investigated<sup>61, 62</sup>. An increase in terms of NO conversion was  
357 reported when methanol was added to the system. Zamansky *et al.* proposed<sup>62</sup> the  
358 addition of a MeOH/H<sub>2</sub>O<sub>2</sub> mixture to further increase the catalytic performance. No more  
359 work related to the methanol promoted NO oxidation has been published as far as we  
360 know. Then, research efforts moved to methanol oxidation in presence of NO. Thus, some  
361 papers<sup>63-65</sup> showed an increase in the MeOH conversion in presence of NO (temperatures



362 from 600 up to 1,200 °C). Furthermore, they proposed a possible mechanism of the  
363 oxidation reaction, concluding that radical formation in presence of NO was occurring.  
364 Since methanol promotes the NO oxidation, we screened different methanol  
365 concentrations to examine our catalysts performance. As far as we know, this is the first  
366 work in which this methodology is applied at room temperature using IL-based catalysts.  
367 Thus, Figure 7 shows the NO conversion as a function of the RH and the methanol  
368 concentration for the 40% ENIL material.

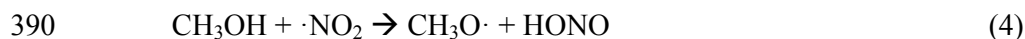
369



370 Figure 7: NO conversion in 40% [bmim][NO<sub>3</sub>] ENIL material with relative  
371 humidity of 10 and 50% and different concentrations of MeOH in the gas phase. Gas  
372 composition: 2,000 ppm NO, 10.5% O<sub>2</sub>, balance N<sub>2</sub>, Flow: 200 mL·min<sup>-1</sup>, GHSV=10,000  
373 h<sup>-1</sup>. Experiments conducted at room temperature.

374 From Figure 7, it can be seen how the NO conversion increases by increasing the  
375 methanol concentration until reaching a maximum. That maximum depends on the RH  
376 studied but it is located at a MeOH/NO ratio between 0.2-0.4 depending on the RH.  
377 Starting with 10% RH, it is clearly seen that NO conversion increases while increasing  
378 the amount of methanol until 400 ppm of MeOH whereafter it remains constant up to  
379 1,600 ppm of MeOH. For 50% RH, the same trend is observed but the maximum is  
380 reached at 800 ppm of MeOH. It seems that for 50% RH, the NO conversion is higher  
381 than at 10% RH at methanol concentrations above 800 ppm. This interesting difference  
382 in the trends might be explained by increased HNO<sub>3</sub> formation when more water is  
383 present in the system (see figure S4 of the Supporting Information). An interesting work  
384 by Xiao *et al.*<sup>66</sup> studying the mechanism of the methanol oxidation in presence of NO  
385 (room temperature performed as well) indicated that NO<sub>2</sub> may play a role in the methanol  
386 oxidation. They proposed a series of intermediate reactions involved in the MeOH

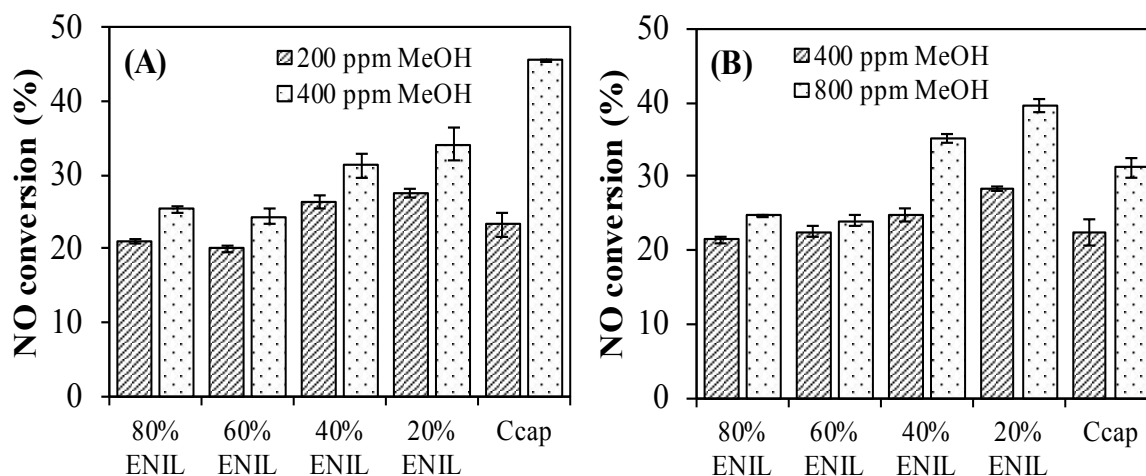
387 oxidation when NO<sub>2</sub> is present. In this context, we believe that two of the proposed  
388 reactions may be occurring in our system:



391 Reactions (3) and (4) may be occurring in our system due to the observed nitrous  
392 acid (HONO) and the absence of NO<sub>2</sub> in the UV-Vis spectrum (see Figure S5 in  
393 Supporting Information), not only while adding the first droplets but also at the steady  
394 state (especially when high conversions were found). This was immediately found when  
395 methanol was added to the system. Furthermore, huge amounts of HNO<sub>3</sub> were detected  
396 while adding MeOH to the system (see Figure S5 in Supporting Information), this may  
397 be explained by the proposed mechanism by Kunov-Kruse *et al.*<sup>28</sup> when using  
398 [bmim][NO<sub>3</sub>] as catalyst in which HNO<sub>3</sub> was formed in the catalytic reaction in presence  
399 of water. In addition, the presence of HONO may lead to fast formation of HNO<sub>3</sub> (due to  
400 nitrous acids well-known instability). Therefore, promoted oxidation of NO in presence  
401 of MeOH may be explained by radical formation in both the liquid and the gas phase.  
402 Low amounts of MeOH that remain absorbed on the IL are simply removed by heating  
403 up the sample to 130 °C. This compound can be easily separated from the others involved  
404 in the reaction due to the high differences in their volatilities. Future works will be  
405 centered on the study of the mechanism of reaction, getting attention the possible other  
406 value-added products formed during the reaction.

407 Based on the optimized MeOH addition, two different concentrations for each RH  
408 (200 and 400 ppm for 10% RH and 400 and 800 ppm for 50% RH) respectively were  
409 selected for testing the different materials.

410



411 Figure 8: NO conversion of the different materials at relative humidity of (A) 10% RH  
 412 and (B) 50% RH and two different concentrations of MeOH in the gas phase. Gas  
 413 composition: 2,000 ppm NO, 10.5% O<sub>2</sub>, balance N<sub>2</sub>, Flow: 200 mL·min<sup>-1</sup>,  
 414 GHSV=10,000 h<sup>-1</sup>. Experiments conducted at room temperature.

415 In

416 Figure 8A, the methanol promoted NO conversions of the different materials at 10%  
 417 RH can be analyzed. In general terms, all the materials exhibit greater conversions with  
 418 the addition of MeOH when compared to the same moisture conditions without MeOH.  
 419 For 200 ppm methanol, it can be seen that the 20% ENIL material presents the highest  
 420 NO conversions while it seems that the amount of MeOH added is not enough for  
 421 overcoming the inhibition in C<sub>Cap</sub> material pores. However, when increasing to 400 ppm  
 422 of MeOH, the hollow carbon capsules exhibit the highest activity. The measurements  
 423 show in general that the addition of methanol promotes the reaction at wet conditions  
 424 independent of the catalyst used.

425

426 Figure 8B shows that the 20% and 40% ENIL materials present the highest  
 427 conversion at 50% RH, even higher than hollow carbon capsules. This suggests that at  
 428 high concentrations of water, the presence of MeOH is not compensating for the  
 429 inhibition of the NO reaction in the C<sub>Cap</sub> material probably due to pore condensation of  
 430 water. The results confirm that for wet conditions with addition of methanol, the ENIL  
 431 materials exhibit a positive effect regarding the NO removal (increase of more than 50%  
 432 in NO conversion when compared to the same moisture conditions without methanol -  
 433 Figure 6).

434 It is important to remark that after testing the performance of each material, TGA  
 435 analysis was performed to check the amount of IL that remains in the support (see Figure  
 436 S6 in Supporting Information) after adding water and methanol to the system. In all cases,  
 437 it was obtained that the same initial amount of IL remained inside the support compared  
 438 to before the catalytic tests.

439 Table 2: NO oxidation performance of different catalysts for dry and wet conditions

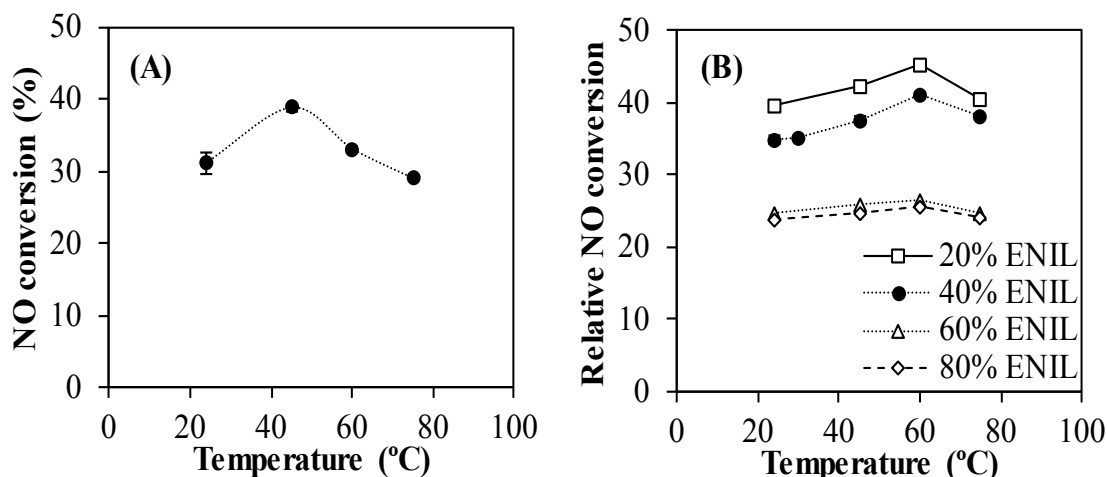
Catalyst	NO dry conversion (%)	NO wet conversion (%)	Ref.
Active carbon	69	0	57
Active carbon	94	0	57
Active carbon nanofibers	73	18	55
Active carbon nanofibers	64	16	55
Active carbon fibers	89	15	56
Porous polymers	43	35	13
Porous polymers	48	31	13

440

441 Table 2 summarizes NO conversion results previously reported in the literature in  
 442 dry and wet conditions. The experimental conditions are close to those used in our work.  
 443 As shown, catalysts based on active carbon present a practically complete inhibition when  
 444 water is added to the system. On the contrary, catalysts based on porous polymers were  
 445 reported as first materials able to oxidize NO in wet conditions, reaching a NO conversion  
 446 of 35%. The difference between ENIL materials and those previously reported is that they  
 447 are not inhibited when water is present in the system, obtaining almost the same NO  
 448 conversion independently of the amount of water. In fact, 40% NO conversion is the  
 449 maximum reached for 20% ENIL catalysts in wet conditions. Therefore, it can be  
 450 concluded that ENIL materials may be an alternative for catalysts typically studied on the  
 451 literature.

#### 452 *Temperature effect on NO conversion*

453 Previous studies reported an increased NO conversion when decreasing the  
 454 temperature (a negative apparent activation energy)<sup>67, 68</sup>, in good agreement with  
 455 homogenous phase oxidation<sup>67</sup>. Figure 9 shows the NO conversion as a function of the  
 456 temperature for the C<sub>Cap</sub> material and the ENIL materials at 50% RH and 800 ppm of  
 457 MeOH.



458 Figure 9: NO conversions in (A) hollow carbon capsules ( $C_{cap}$ ) and (B) ENIL materials  
 459 as a function of the temperature using 50% Relative Humidity and 800 ppm of MeOH in  
 460 the gas phase. Gas composition: 2,000 ppm NO, 10.5% O<sub>2</sub>, balance N<sub>2</sub>, Flow: 200  
 461 mL·min<sup>-1</sup>, GHSV=10,000 h<sup>-1</sup>.

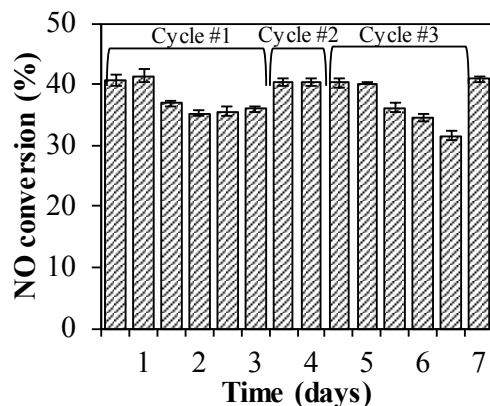
462 As shown in Figure 9A, the  $C_{cap}$  material optimum was found at 45 °C while in the  
 463 case of the ENIL material (Figure 9B), the maximum is located at 60 °C. In the case of  
 464 the ENIL material, the maximum at 60 °C may be attributed to the competing limitations  
 465 (radical formation) at low temperature and the lower gas solubility in the IL at higher  
 466 temperatures. These conclusions concern the 20 and 40% ENIL materials in which most  
 467 of the IL seems to be accessible to the gas, contrary to the 60 and 80% ENILs, where the  
 468 temperature does not affect the NO conversion. The different temperature effect observed  
 469 on  $C_{cap}$  and ENIL materials may be caused by the place in which the reaction is occurring,  
 470 i.e pores of  $C_{cap}$  and IL of ENIL materials. Moreover, it may be easier to retain the  
 471 absorbed gas on the liquid media than on pores of solid material when temperature is  
 472 increased. However, in general, the impact of the temperature on the NO conversion is  
 473 not very important, reaching about 25% at maximum.

474 It can be concluded that the oxidation at higher temperatures (approaching flue gas  
 475 stack temperatures) results in a slight increment of NO conversion, i.e. at temperatures  
 476 close to 60 °C, the NO conversion is in the range of 45%, in presence of water in the gas  
 477 phase.

478

479

480



481

482 Figure 10: Stability measurements using 20% ENIL material using 50% Relative  
483 Humidity and 800 ppm of MeOH in the gas phase. Gas composition: 2,000 ppm  
484 NO, 10.5% O<sub>2</sub>, balance N<sub>2</sub>, Flow: 200 mL·min<sup>-1</sup>, GHSV=10,000 h<sup>-1</sup>.

485 Figure 10 presents the stability measurements of 20% ENIL material in four  
486 different cycles. As can be seen, NO conversion is maintained for 24 hours. Then, it  
487 started to decrease due to the IL saturation by NO<sub>x</sub> and HNO<sub>3</sub> formed. The increase in  
488 the temperature up to 130 °C allows the complete regeneration of the catalyst reaching  
489 the same values of the fresh one. Therefore, it was demonstrated one day stability and the  
490 easy regeneration of the catalyst by a simple temperature increase.

491 Encapsulated Ionic Liquids (ENILs) were successfully applied as catalysts for NO  
492 oxidation at low temperatures. ENILs with different loads of the IL [bmim][NO<sub>3</sub>] were  
493 synthesized and then characterized by means of elemental analysis, thermal stability,  
494 porous structure and microscopy. Experiments in dry gas show higher NO conversion of  
495 the hollow carbon capsules compared to ENILs, where the conversion increased with  
496 decreasing the IL loading. Experiments conducted at different relative humidities showed  
497 positive effect on NO conversion for the ENIL materials. On the contrary, the results of  
498 empty carbon material showed inhibition of the NO oxidation by increasing humidity in  
499 the system. The reaction was promoted (in presence of water) by addition of methanol to  
500 the system. The amount of methanol added to the system was optimized (at different RH),  
501 showing an optimal MeOH/NO ratio between 0.2-0.4. In this case, ENILs composed of  
502 20 and 40% of IL exhibited the greatest performance (including hollow carbon capsules)  
503 reaching conversions near 45%. The temperature effect on the reaction revealed an  
504 optimum temperature of 60 °C when using ENILs, accomplishing relative NO  
505 conversions 20% higher than at room temperature ones. Stability measurements revealed

506 NO conversion is maintained during at least 24 h without any loss. The catalyst was easily  
507 regenerated by increasing the temperature up to 130 °C. These results demonstrate  
508 potential application of ENILs as catalysts at near industrial flue gas conditions to create  
509 “fast SCR” for a down-stream traditional SCR catalyst.

510 **Supporting Information:** Elemental composition characterization of ENIL  
511 materials involved in the work. Pore size distribution of the materials involved in the  
512 work. N<sub>2</sub> adsorption/desorption isotherms @ 77 K of all the materials involved in the  
513 work. UV-Vis Spectrum of hollow carbon capsules (C<sub>Cap</sub>) in dry conditions at different  
514 oxygen contents. UV-Vis Spectrum of 40% [bmim][NO<sub>3</sub>] ENIL material (40% ENIL) in  
515 dry and 10% Relative Humidity conditions. UV-Vis Spectrum of 20% [bmim][NO<sub>3</sub>]  
516 ENIL material (20% ENIL) in 50% Relative Humidity and 800 ppm of MeOH conditions.  
517 TGA analysis of the materials used in this work: hollow carbon capsules (C<sub>Cap</sub>) and ENIL  
518 materials with four different IL loads (20, 40, 60 and 80 % of [bmim][NO<sub>3</sub>]) after being  
519 used in the catalytic reactions.

## 520 Acknowledgments

521 The authors thank the Ministerio de Economía y Competitividad (MINECO) of  
522 Spain (project CTQ2017-89441-R) and Comunidad de Madrid (P2018/EMT4348) for  
523 financial support. Rubén Santiago also thanks David Nielsen for his great support at DTU.

## 524 References

- 525 1. Chang, S. G.; Liu, D. K., Removal of nitrogen and sulphur oxides from waste gas  
526 using a phosphorus/alkali emulsion. *Nature* **1990**, *343*, 151.
- 527 2. Pham, E. K.; Chang, S.-G., Removal of NO from flue gases by absorption to an  
528 iron(ii) thiochelatate complex and subsequent reduction to ammonia. *Nature* **1994**, *369*,  
529 139.
- 530 3. Kanchongkittiphon, W.; Mendell, M. J.; Gaffin, J. M.; Wang, G.; Phipatanakul,  
531 W., Indoor Environmental Exposures and Exacerbation of Asthma: An Update to the  
532 2000 Review by the Institute of Medicine. *Environmental Health Perspectives* **2015**, *123*  
533 (1), 6-20.
- 534 4. Solomon, S., Stratospheric ozone depletion: A review of concepts and history.  
535 *Reviews of Geophysics* **1999**, *37* (3), 275-316.
- 536 5. Volz, A.; Kley, D., Evaluation of the Montsouris series of ozone measurements  
537 made in the nineteenth century. *Nature* **1988**, *332*, 240.
- 538 6. Liu, N.; Lu, B.-H.; Zhang, S.-H.; Jiang, J.-L.; Cai, L.-L.; Li, W.; He, Y.,  
539 Evaluation of Nitric Oxide Removal from Simulated Flue Gas by  
540 Fe(II)EDTA/Fe(II)citrate Mixed Absorbents. *Energy & Fuels* **2012**, *26* (8), 4910-4916.
- 541 7. Jirat, J.; Stepanek, F.; Marek, M.; Kubicek, M., Comparison of design and  
542 operation strategies for temperature control during selective catalytic reduction of NOx.  
543 *Chemical Engineering & Technology* **2001**, *24* (1), 35-40.

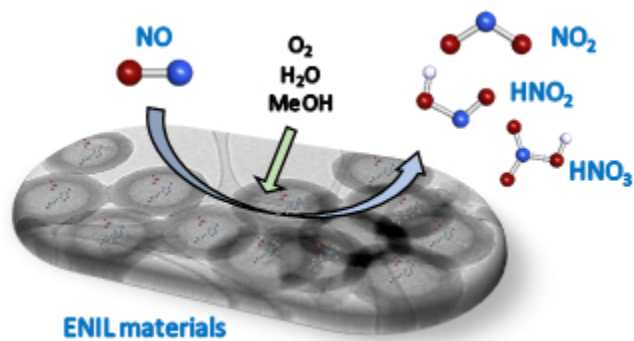
- 544 8. Maisuls, S. E.; Seshan, K.; Feast, S.; Lercher, J. A., Selective catalytic reduction  
545 of NO<sub>x</sub> to nitrogen over Co-Pt/ZSM-5: Part A. Characterization and kinetic studies.  
546 *Applied Catalysis B: Environmental* **2001**, *29* (1), 69-81.
- 547 9. Gao, Y.; Luan, T.; LÜ, T.; Cheng, K.; Xu, H., Performance of V<sub>2</sub>O<sub>5</sub>-WO<sub>3</sub>-  
548 MoO<sub>3</sub>/TiO<sub>2</sub> Catalyst for Selective Catalytic Reduction of NO<sub>x</sub> by NH<sub>3</sub>. *Chinese Journal*  
549 *of Chemical Engineering* **2013**, *21* (1), 1-7.
- 550 10. Busca, G.; Lietti, L.; Ramis, G.; Berti, F., Chemical and mechanistic aspects of  
551 the selective catalytic reduction of NO<sub>x</sub> by ammonia over oxide catalysts: A review.  
552 *Applied Catalysis B: Environmental* **1998**, *18* (1), 1-36.
- 553 11. Zhang, Z.; Atkinson, J. D.; Jiang, B.; Rood, M. J.; Yan, Z., NO oxidation by  
554 microporous zeolites: Isolating the impact of pore structure to predict NO conversion.  
555 *Applied Catalysis B: Environmental* **2015**, *163*, 573-583.
- 556 12. Zhang, Z.; Atkinson, J. D.; Jiang, B.; Rood, M. J.; Yan, Z., Nitric oxide oxidation  
557 catalyzed by microporous activated carbon fiber cloth: An updated reaction mechanism.  
558 *Applied Catalysis B: Environmental* **2014**, *148-149*, 573-581.
- 559 13. Ghafari, M.; Atkinson, J. D., Catalytic NO Oxidation in the Presence of Moisture  
560 Using Porous Polymers and Activated Carbon. *Environ Sci Technol* **2016**, *50* (10), 5189-  
561 5196.
- 562 14. Long, X. L.; Xin, Z. L.; Chen, M. B.; Xiao, W. D.; Yuan, W. K., Nitric oxide  
563 absorption into cobalt ethylenediamine solution. *Separation and Purification Technology*  
564 **2007**, *55* (2), 226-231.
- 565 15. Khan, N. E.; Adewuyi, Y. G., Absorption and Oxidation of Nitric Oxide (NO) by  
566 Aqueous Solutions of Sodium Persulfate in a Bubble Column Reactor. *Industrial &*  
567 *Engineering Chemistry Research* **2010**, *49* (18), 8749-8760.
- 568 16. Demmink, J. F.; van Gils, I. C. F.; Beenackers, A. A. C. M., Absorption of Nitric  
569 Oxide into Aqueous Solutions of Ferrous Chelates Accompanied by Instantaneous  
570 Reaction. *Industrial & Engineering Chemistry Research* **1997**, *36* (11), 4914-4927.
- 571 17. Chien, T. W.; Hsueh, H. T.; Chu, B. Y.; Chu, H., Absorption kinetics of NO from  
572 simulated flue gas using Fe(II)EDTA solutions. *Process Safety and Environmental*  
573 *Protection* **2009**, *87* (5), 300-306.
- 574 18. Zhu, H.-S.; Mao, Y.-P.; Chen, Y.; Long, X.-L.; Yuan, W.-K., Removal of nitric  
575 oxide and sulfur dioxide from flue gases using a FeII-ethylenediamineteraacetate  
576 solution. *Korean Journal of Chemical Engineering* **2013**, *30* (6), 1241-1247.
- 577 19. Welton, T., Ionic liquids: a brief history. *Biophys Rev* **2018**, *10*, 691-706.
- 578 20. Kosmulski, M.; Gustafsson, J.; Rosenholm, J. B., Thermal stability of low  
579 temperature ionic liquids revisited. *Thermochimica Acta* **2004**, *412* (1), 47-53.
- 580 21. Aghaie, M.; Rezaei, N.; Zendejboudi, S., A systematic review on CO<sub>2</sub> capture  
581 with ionic liquids: Current status and future prospects. *Renewable & Sustainable Energy*  
582 *Reviews* **2018**, *96*, 502-525.
- 583 22. Lin, H.; Bai, P.; Guo, X. H., Ionic Liquids for SO<sub>2</sub> Capture: Development and  
584 Progress. *Asian J. Chem.* **2014**, *26* (9), 2501-2506.
- 585 23. Wang, L. Y.; Xu, Y. L.; Li, Z. D.; Wei, Y. N.; Wei, J. P., CO<sub>2</sub>/CH<sub>4</sub> and  
586 H<sub>2</sub>S/CO<sub>2</sub> Selectivity by Ionic Liquids in Natural Gas Sweetening. *Energy & Fuels* **2018**,  
587 *32* (1), 10-23.
- 588 24. Bedia, J.; Palomar, J.; Gonzalez-Miquel, M.; Rodriguez, F.; Rodriguez, J. J.,  
589 Screening ionic liquids as suitable ammonia absorbents on the basis of thermodynamic  
590 and kinetic analysis. *Separation and Purification Technology* **2012**, *95*, 188-195.
- 591 25. Bedia, J.; Ruiz, E.; de Riva, J.; Ferro, V. R.; Palomar, J.; Jose Rodriguez, J.,  
592 Optimized Ionic Liquids for Toluene Absorption. *AIChE J.* **2013**, *59* (5), 1648-1656.



- 593 26. Chen, K. H.; Shi, G. L.; Zhou, X. Y.; Li, H. R.; Wang, C. M., Highly Efficient  
594 Nitric Oxide Capture by Azole-Based Ionic Liquids through Multiple-Site Absorption.  
595 *Angewandte Chemie-International Edition* **2016**, *55* (46), 14362-14366.
- 596 27. Sun, Y.; Ren, S.; Hou, Y.; Zhang, K.; Wu, W., Absorption of nitric oxide in  
597 simulated flue gas by a metallic functional ionic liquid. *Fuel Processing Technology*  
598 **2018**, *178*, 7-12.
- 599 28. Kunov-Kruse, A. J.; Thomassen, P. L.; Riisager, A.; Mossin, S.; Fehrmann, R.,  
600 Absorption and Oxidation of Nitrogen Oxide in Ionic Liquids. *Chemistry-a European*  
601 *Journal* **2016**, *22* (33), 11745-11755.
- 602 29. Hu, Z. H.; Margulis, C. J., Room-temperature ionic liquids: Slow dynamics,  
603 viscosity, and the red edge effect. *Accounts Chem. Res.* **2007**, *40* (11), 1097-1105.
- 604 30. Santiago, R.; Lemus, J.; Moreno, D.; Moya, C.; Larriba, M.; Alonso-Morales,  
605 N.; Gilarranz, M. A.; Rodriguez, J. J.; Palomar, J., From kinetics to equilibrium control  
606 in CO<sub>2</sub> capture columns using Encapsulated Ionic Liquids (ENILs). *Chemical*  
607 *Engineering Journal* **2018**, *348*, 661-668.
- 608 31. Palomar, J.; Lemus, J.; Alonso-Morales, N.; Bedia, J.; Gilarranz, M. A.;  
609 Rodriguez, J. J., Encapsulated ionic liquids (ENILs): from continuous to discrete liquid  
610 phase. *Chemical Communications* **2012**, *48* (80), 10046-10048.
- 611 32. Lemus, J.; Palomar, J.; A. Gilarranz, M.; J. Rodriguez, J., Characterization of  
612 Supported Ionic Liquid Phase (SILP) materials prepared from different supports.  
613 *Adsorption* **2011**, *17*, 561-571.
- 614 33. Thomassen, P.; Kunov-Kruse, A. J.; Mossin, S.; Kolding, H.; Kegns, S.;  
615 Riisager, A.; Fehrmann, R., Separation of Flue Gas Components by SILP (Supported  
616 Ionic Liquid-Phase) Absorbers. In *Molten Salts and Ionic Liquids 18*, Reichert, W. M.;  
617 Mantz, R. A.; Trulove, P. C.; Ispas, A.; Fox, D. M.; Mizuhata, M.; DeLong, H. C.;  
618 Bund, A., Eds. 2012; Vol. 50, pp 433-442.
- 619 34. Mehnert, C. P.; Cook, R. A.; Dispenziere, N. C.; Afeworki, M., Supported Ionic  
620 Liquid Catalysis – A New Concept for Homogeneous Hydroformylation Catalysis.  
621 *Journal of the American Chemical Society* **2002**, *124* (44), 12932-12933.
- 622 35. Riisager, A.; Fehrmann, R.; Haumann, M.; Wasserscheid, P., Supported Ionic  
623 Liquid Phase (SILP) catalysis: An innovative concept for homogeneous catalysis in  
624 continuous fixed-bed reactors. *European Journal of Inorganic Chemistry* **2006**, (4), 695-  
625 706.
- 626 36. Fehrmann, R.; Riisager, A.; Haumann, M., *Supported Ionic Liquids:*  
627 *Fundamentals and Applications*. 2014; p 1-474.
- 628 37. Romanos, G. E.; Schulz, P. S.; Bahlmann, M.; Wasserscheid, P.; Sapalidis, A.;  
629 Katsaros, F. K.; Athanasekou, C. P.; Beltsios, K.; Kanellopoulos, N. K., CO<sub>2</sub> Capture  
630 by Novel Supported Ionic Liquid Phase Systems Consisting of Silica Nanoparticles  
631 Encapsulating Amine-Functionalized Ionic Liquids. *The Journal of Physical Chemistry*  
632 *C* **2014**, *118* (42), 24437-24451.
- 633 38. Riisager, A.; Jørgensen, B.; Wasserscheid, P.; Fehrmann, R., First application of  
634 supported ionic liquid phase (SILP) catalysis for continuous methanol carbonylation.  
635 *Chemical Communications* **2006**, (9), 994-996.
- 636 39. Wang, H. B.; Hu, Y.-L.; Li, D.-J., Facile and efficient Suzuki–Miyaura coupling  
637 reaction of aryl halides catalyzed by Pd<sub>2</sub>(dba)<sub>3</sub> in ionic liquid/supercritical carbon  
638 dioxide biphasic system. *J. Mol. Liq.* **2016**, *218*, 429-433.
- 639 40. Hu, Y. L.; Wu, Y. P.; Lu, M., Co (II)-C12 alkyl carbon chain multi-functional  
640 ionic liquid immobilized on nano-SiO<sub>2</sub> nano-SiO<sub>2</sub>@CoCl<sub>3</sub>-C12IL as an efficient  
641 cooperative catalyst for C–H activation by direct acylation of aryl halides with aldehydes.  
642 *Appl. Organomet. Chem.* **2018**, *32* (2), e4096.

- 643 41. Yao, N.; Lu, M.; Liu, X. B.; Tan, J.; Hu, Y. L., Copper-doped mesoporous silica  
644 supported dual acidic ionic liquid as an efficient and cooperative reusability catalyst for  
645 Biginelli reaction. *J. Mol. Liq.* **2018**, *262*, 328-335.
- 646 42. Hu, Y. L.; Zhang, R. L.; Fang, D., Quaternary phosphonium cationic ionic  
647 liquid/porous metal-organic framework as an efficient catalytic system for cycloaddition  
648 of carbon dioxide into cyclic carbonates. *Environmental Chemistry Letters* **2019**, *17* (1),  
649 501-508.
- 650 43. Jin, T.; Dong, F.; Liu, Y.; Hu, Y. L., Novel and effective strategy of dual bis  
651 (trifluoromethylsulfonyl) imide imidazolium ionic liquid immobilized on periodic  
652 mesoporous organosilica for greener cycloaddition of carbon dioxide to epoxides. *New J.*  
653 *Chem.* **2019**, *43* (6), 2583-2590.
- 654 44. Lemus, J.; Bedia, J.; Moya, C.; Alonso-Morales, N.; A Gilarranz, M.; Palomar,  
655 J.; J Rodriguez, J., Ammonia Capture from Gas Phase by Encapsulated Ionic Liquids  
656 (ENILs). *RSC Advances* **2016**, *6*, 61650-61660.
- 657 45. Lemus, J.; Da Silva, F. A. F.; Palomar, J.; Carvalho, P. J.; Coutinho, J. A. P.,  
658 Solubility of carbon dioxide in encapsulated ionic liquids. *Separation and Purification*  
659 *Technology* **2018**, *196*, 41-46.
- 660 46. Moya, C.; Alonso-Morales, N.; Gilarranz, M. A.; Rodriguez, J. J.; Palomar, J.,  
661 Encapsulated Ionic Liquids for CO<sub>2</sub> Capture: Using 1-Butyl-methylimidazolium Acetate  
662 for Quick and Reversible CO<sub>2</sub> Chemical Absorption. *Chemphyschem* **2016**, *17* (23),  
663 3891-3899.
- 664 47. Moya, C.; Alonso-Morales, N.; de Riva, J.; Morales-Collazo, O.; Brennecke, J.  
665 F.; Palomar, J., Encapsulation of Ionic Liquids with an Aprotic Heterocyclic Anion  
666 (AHA-IL) for CO<sub>2</sub> Capture: Preserving the Favorable Thermodynamics and Enhancing  
667 the Kinetics of Absorption. *The Journal of Physical Chemistry B* **2018**, *122* (9), 2616-  
668 2626.
- 669 48. Santiago, R.; Lemus, J.; Moya, C.; Moreno, D.; Alonso-Morales, N.; Palomar,  
670 J., Encapsulated Ionic Liquids to Enable the Practical Application of Amino Acid-Based  
671 Ionic Liquids in CO<sub>2</sub> Capture. *ACS Sustainable Chemistry & Engineering* **2018**, *6* (11),  
672 14178-14187.
- 673 49. Buchel, G.; Unger, K. K.; Matsumoto, A.; Tsutsumi, K., A novel pathway for  
674 synthesis of submicrometer-size solid core/mesoporous shell silica spheres. *Advanced*  
675 *Materials* **1998**, *10* (13), 1036-1038.
- 676 50. Alonso-Morales, N.; Gilarranz, M. A.; Palomar, J.; Lemus, J.; Heras, F.;  
677 Rodriguez, J. J., Preparation of hollow submicrocapsules with a mesoporous carbon shell.  
678 *Carbon* **2013**, *59*, 430-438.
- 679 51. Alonso-Morales, N.; Ruiz-Garcia, C.; Palomar, J.; Heras, F.; Calvo, L.;  
680 Rodriguez, J. J.; Gilarranz, M. A., Hollow Nitrogen- or Boron-Doped Carbon  
681 Submicrospheres with a Porous Shell: Preparation and Application as Supports for  
682 Hydrodechlorination Catalysts. *Industrial & Engineering Chemistry Research* **2017**, *56*  
683 (27), 7665-7674.
- 684 52. Baukal, C. E.; Eleazer, P. B., Quantifying NO<sub>x</sub> for Industrial Combustion  
685 Processes. *Journal of the Air & Waste Management Association* **1998**, *48* (1), 52-58.
- 686 53. Sousa, J. P. S.; Pereira, M. F. R.; Figueiredo, J. L., NO oxidation over nitrogen  
687 doped carbon xerogels. *Applied Catalysis B: Environmental* **2012**, *125*, 398-408.
- 688 54. Kunov-Kruse, A. J.; Thomassen, P.; Mossin, S. L.; Riisager, A.; Fehrmann, R.,  
689 Absorption and oxidation of NO in 1-butyl-3-methylimidazolium based ionic liquids -  
690 mechanism of reaction. *Abstracts of Papers of the American Chemical Society* **2014**, *247*.

- 691 55. Mochida, I.; Kismori, S.; Hironaka, M.; Kawano, S.; Matsumura, Y.;  
692 Yoshikawa, M., Oxidation of NO into NO<sub>2</sub> over Active Carbon Fibers. *Energy & Fuels*  
693 **1994**, *8* (6), 1341-1344.
- 694 56. Mochida, I.; Kawabuchi, Y.; Kawano, S.; Matsumura, Y.; Yoshikawa, M., High  
695 catalytic activity of pitch-based activated carbon fibres of moderate surface area for  
696 oxidation of NO to NO<sub>2</sub> at room temperature. *Fuel* **1997**, *76* (6), 543-548.
- 697 57. Guo, Z.; Xie, Y.; Hong, I.; Kim, J., *Catalytic oxidation of NO to NO<sub>2</sub> on activated*  
698 *carbon*. 2001; Vol. 42, p 2005-2018.
- 699 58. Ruggeri, M. P.; Nova, I.; Tronconi, E., Experimental Study of the NO Oxidation  
700 to NO<sub>2</sub> Over Metal Promoted Zeolites Aimed at the Identification of the Standard SCR  
701 Rate Determining Step. *Top. Catal.* **2013**, *56* (1), 109-113.
- 702 59. Atkins, P.; de Paula, J., *Atkins' Physical Chemistry*. 9th ed.; OUP Oxford: 2010.
- 703 60. Hubbe, M.; D Smith, R.; Zou, X.; Katuscak, S.; Potthast, A.; Ahn, K.,  
704 *Deacidification of Acidic Books and Paper by Means of Non-aqueous Dispersions of*  
705 *Alkaline Particles: A Review Focusing on Completeness of the Reaction*. 2017; Vol. 12,  
706 p 4410-4477.
- 707 61. Lyon, R. K.; Cole, J. A.; Kramlich, J. C.; Chen, S. L., The selective reduction of  
708 SO<sub>3</sub> to SO<sub>2</sub> and the oxidation of NO to NO<sub>2</sub> by methanol. *Combustion and Flame -*  
709 *COMBUST FLAME* **1990**, *81* (1), 30-39.
- 710 62. Zamansky, V. M.; Ho, L. O. C.; Maly, P. M.; Seeker, W. R., Oxidation of NO to  
711 NO<sub>2</sub> by Hydrogen Peroxide and its Mixtures with Methanol in Natural Gas and Coal  
712 Combustion Gases. *Combust. Sci. Technol.* **1996**, *120* (1-6), 255-272.
- 713 63. Rasmussen, C. L.; Wassard, K. H.; Dam-Johansen, K.; Glarborg, P., Methanol  
714 oxidation in a flow reactor: Implications for the branching ratio of the CH<sub>3</sub>OH+ OH  
715 reaction. *International Journal of Chemical Kinetics* **2008**, *40* (7), 423-441.
- 716 64. Taylor, P.; Cheng, L.; Dellinger, B., The influence of nitric oxide on the oxidation  
717 of methanol and ethanol. *Combustion and Flame - COMBUST FLAME* **1998**, *115*, 561-  
718 567.
- 719 65. Alzueta, M. U.; Bilbao, R.; Finestra, M., Methanol Oxidation and Its Interaction  
720 with Nitric Oxide. *Energy & Fuels* **2001**, *15* (3), 724-729.
- 721 66. Xiao, C.-X.; Yan, N.; Zou, M.; Hou, S.-C.; Kou, Y.; Liu, W.; Zhang, S., NO<sub>2</sub>-  
722 catalyzed deep oxidation of methanol: Experimental and theoretical studies. *Journal of*  
723 *Molecular Catalysis A: Chemical* **2006**, *252* (1), 202-211.
- 724 67. Artioli, N.; Lobo, R. F.; Iglesia, E., Catalysis by Confinement: Enthalpic  
725 Stabilization of NO Oxidation Transition States by Microporous and Mesoporous  
726 Siliceous Materials. *The Journal of Physical Chemistry C* **2013**, *117* (40), 20666-20674.
- 727 68. Loiland, J. A.; Lobo, R. F., Low temperature catalytic NO oxidation over  
728 microporous materials. *Journal of Catalysis* **2014**, *311*, 412-423.



Methanol promoted oxidation of NO using Encapsulated Ionic Liquids (ENILs)

84x47mm (96 x 96 DPI)